IJCRT.ORG ISSN : 2320-2882

INTERNATIONAL JOURNAL OF CREATIVE RESEARCH THOUGHTS (IJCRT)

An International Open Access, Peer-reviewed, Refereed Journal

Quantitative Structure Activity Relationship Studies Of Darunavir And Their Derivatives As HIV-1 Protease Inhibitors

Pandarinathan. S[1] and Jayanthi. S[2*]

[1]Agricultural College and Research Institute [TNAU], Vazhavachanur-606753, Tamil Nadu, India

[2]Shri Sakthikailassh Women's College, Salem-636003, Tamil Nadu, India

*Corresponding author

S. Jayanthi

Shri Sakthikailassh Women's College, Military Road, Ammapet, Salem-636003. Tamil Nadu, India

Abstract

The design of potent inhibitors against human immunodeficiency virus type-1 protease (HIV-1 PR) remains a central strategy in antiretroviral drug discovery. Here, we report an integrated ligand-based and structure-based computational approach to explore the activity landscape of darunavir and 43 structurally diverse derivatives (compounds 1–44). Experimental activity data (IC_{50} = 0.01–1 µM; Ki = 0.005–0.243 nM), obtained from the Binding Database, were transformed into a negative logarithmic scale and employed for quantitative structure–activity relationship (QSAR) modeling. Ligands were preprocessed using LigPrep with the OPLS-2005 force field, followed by alignment to ensure consistency in model development. Robust predictive models were generated using the AutoQSAR framework, which integrates machine-learning algorithms with molecular fingerprints and physicochemical descriptors. The dataset was randomly divided into a training set (70%) and a test set (30%). Kernel-PLS visualization provided atomic-level insights, highlighting favorable and unfavorable contributions to activity. Complementary 3D-QSAR models were developed using a Gaussian-based grid approach, where steric, electrostatic, hydrophobic, and hydrogen-bond fields were evaluated. Models with acceptable statistical performance ($0.5 < R^2 < 1$) were retained for interpretation. To validate the QSAR findings, molecular docking was performed using the Glide XP protocol against HIV-1 PR (PDB ID: 4HLA). Darunavir, compound-32, and compound-33 demonstrated favorable binding conformations within the protease active site, supported by GlideScore evaluations. Together, these findings underscore the synergy of QSAR modeling and docking simulations in elucidating structural determinants of HIV-1 PR inhibition and highlight promising scaffolds for the rational design of next-generation protease inhibitors.

1. Introduction

Over the past few years, there has been significant progress in the development of highly active antiretroviral therapies to combat human immunodeficiency virus type 1 [1]. These therapies have demonstrated exceptional effectiveness in reducing viral load and significantly slowing down the progression of the disease [1]. On the other hand, the development of resistance to medication for the HIV variants poses a growing threat and necessitates the urgent development of novel anti-HIV agents. The catalytic activity of viral protease facilitates the conversion of an immature viron, which is non-infectious, into a fully developed infectious virus [2]. Consequently, the HIV-1 protease holds great potential as a target for the design of anti-HIV-1 protease [3]. In 2016, the Office of AIDS Research Advisory Council brought up Darunavir as a treatment option among other licensed protease inhibitors such as Tipranavir, Ritonavir, Lopinavir, Nelfinavir, Atzanavir, Indinavir, Amprenavir, and Saquinavir. One particularly interesting group of inhibitors is darunavir and its similar compounds, which offer a wide range of activities and structural diversity, making them suitable for computational investigations [4]. However, there is currently very little information regarding the specific structural features necessary to elicit the inhibitory action. In order to comprehend the structural characteristics of HIV-1 protease, we will construct three-dimensional quantitative structural activity relationship (3D-QSAR) models. These models offer an advantage over 1D and 2D QSAR methods as they provide meaningful information about pharmacophore features that are relevant to the activity. An essential concept in QSAR is the domain of the application which is used to evaluate the level of uncertainty in predicting the activity of specific molecule based on its similarity to the compounds used to create the model. In recent years, there has been an increase in the number of QSAR models based on large and diverse datasets [5]. By employing robust statistical analysis, 3D-QSAR aids in elucidating the 3D properties of ligands and predicting their biological activities. In recent years, the quantitative structure-activity relationship (QSAR) approach has gained immense popularity for modelling the chemical and biological properties of small molecules [6]. This approach has numerous advantages, such as cost-effectiveness and high productivity in modelling large chemical libraries. Moreover, it enables the evaluation of properties of compounds that are yet to be synthesized or do not exist. These benefits are especially valuable in the field of drug design and discovery. Numerous investigations have been conducted on the subject of HIV-1 protease inhibitors, employing both two-dimensional (2D) and three-dimensional (3D) quantitative structure-activity relationship (QSAR) methodologies [7-12]. Prior QSAR models have highlighted the significance of various molecular attributes, including size, shape, hydrophobicity, hydrogen bonds, molecular connectivity, and charge distribution, in accurately predicting the biological activity of these inhibitors [13]. The QSAR studies have carried out of anti-HIV compound with the correlation of optimum logP values [14], non-linear transformation of descriptors with biological activity [13], cyclic urea-based HIV-1 protease inhibitors [15], carboxamide derivatives [16], tetrahydropyrimidine-2-one protease inhibitors [17], Tipranavir analogs [18], Chromone Derivatives [19], and fullerene-based protease inhibitors [20]. Therefore, within this chapter, we have conducted 3D-QSAR analysis on darunavir and their derivatives, which have been validated through statistical analysis. Additionally, the fitness of binding, comparative binding affinities, and the interactions between HIV-1 protease and darunavir derivatives will be identified through molecular docking.

2. Computational methodology

Dataset, training set and test set: A variety of structurally diverse darunavir and its derivatives (1-44) with a wide range of HIV-1 protease activities (IC50=0.01-1μM) were chosen from the binding database [21]. These molecules exhibited a uniform distribution of Ki values within the range of 0.005-0.243nM which were then selected for further analysis. The chemical structures of these inhibitors and their experimental activities were converted to a negative logarithmic scale using Maestro's calculator tool, referred to as *activity*. To create a dataset for training and testing, the 3D-gaussian based QSAR of Maestro's random selection tool was utilized. After the cleaning process, the chosen molecules underwent processing with *LigPrep* software. The OPLS-2005 force field was utilized for this purpose, with the desalt option being deactivated. Subsequently, one low-energy ring conformation per ligand was generated, and the ligands were prepared for refinement prior to the development of the QSAR model. Further, the dataset was aligned using the alignment tool that allows the successful generation of QSAR model (**Figure 1**).

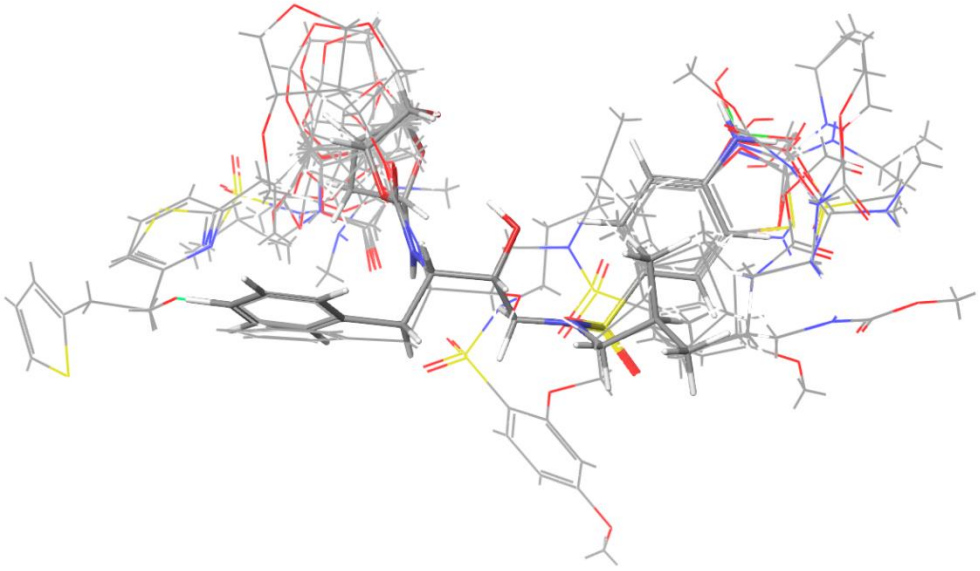

Figure 1: Superimposition of aligned compounds (1-44), darunavir shown in stick and other molecules are shown in line.

AutoQSAR and 3D-QSAR model: It is crucial to identify suitable training and test sets in order to effectively generate predictive QSAR models, especially for diverse compound collections that require constant iteration until a satisfactory QSAR model is obtained. In this study, we employed an AutoQSAR application to create fingerprint-based machine-learning models that automatically generate various physicochemical and topological descriptors. The ligands and their corresponding activities were extracted from the project table and subsequently assessed using machine-learning algorithms. The training set was randomly generated, encompassing 70% of the dataset while 30% was set aside for testing. We utilized the kernel-PLS visualization method to associate the atomic contributions from the QSAR model obtained through the AutoQSAR module with the biological property. This method is a predictive model that enables the identification of positive and negative contributions of individual atoms towards activity, making it easier to visualize the results. Additionally, 3D-QSAR models were generated with a grid spacing of 0.1Å, extending the grid by 3.0Å beyond the limits of the training set. This was achieved using the Gaussian-based approach provided by the Maestro program. To ensure accuracy, force field values within 2.0Å of any training set atom were ignored. The steric, electrostatic, hydrophobic, HBA, HBD force field was truncated at 30kcal/mol. Variables with a standard deviation <0.01 were eliminated, and the optimal models were chosen based on their R^2 values (value should be $1< r^2 > 0.5$).

Molecular Docking: Ligand structures of darunavir, compound-32, and compound-33 were prepared using the *LigPrep* module in Schrödinger Suite (**Schrödinger Release 2023-3**: Glide, Schrödinger, LLC, New York, NY, 2023). This process generated high-quality, all-atom 3D conformations through 2D–3D conversion, stereoisomer/tautomer generation, structural correction, and energy minimization. The receptor model was built using the HIV-1 protease enzyme (PDB ID: 4HLA), for which the active-site residues were defined to guide docking. A receptor grid was generated with the *Receptor Grid Generation* tool in Glide. Docking simulations were performed using the Glide XP (Extra Precision) protocol, which accounts for detailed energetic contributions to enhance accuracy in binding predictions. The docked poses were ranked according to the GlideScore (G-Score) scoring function.

3. Results and Discussion

In recent years, computer-aided drug design has emerged as a prominent field of research with vast applications. This innovative approach enables us to computationally screen biologically active compounds, leading to significant advancements. To enhance the drug-like properties and gain insights into the physiochemical and topological characteristics of darunavir and its derivatives, comprehensive 2D and 3D-QSAR studies were conducted. In the present study, we have used a combination of 2D-QSAR with atomic contribution visualization to improve the QSAR efficiency followed by 3D-QSAR model. According to the reports, darunavir and its derivatives have shown biological activity against HIV-1 protease, with a narrow range of activity values. We have collected a total of 44 molecules, including darunavir, to create QSAR models (**Table 1**). To develop these models, it is essential to have

a minimum of three logarithmic scales of activity range for selected derivatives. QSAR method is used to explain the properties of various molecules, such as topologic, electronic, steric, and hydrophobic, and it is determined through both experimental and computational methods. The AutoQSAR method generated a variety of 2D models that enable the optimal selection of compounds for both the training and test sets, resulting in high-quality models [22]. The most outstanding QSAR models, based on Kernel PLS with molprint2D, linear, and dendritic fingerprints, are presented in **Table 2**. When determining the best model, we prioritized the highest score as the primary criterion, followed by q^2 (predicted activity for the test set) and r^2 (coefficient for the training set). Utilizing a linear Kernel PLS model (PLS=4) with 70% of the dataset for training, we obtained a score of 0.8739 and a q^2 value of 8519. In contrast, the KPLS model with molprint2D method yielded a score of 0.8681 and a q^2 value of 0.8739. Given that the score values reflect the correlation between the training and test sets, we relied on these statistical parameters to identify the most optimal 2D model. **Figure 2** shows the observed and predicted activity of the both models which represents a close agreement of fitting points on the regression line. Similarly, the Gaussian-based 3D-QSAR model shows that the models PLS-2 and PLS-3 have acceptable r^2 values; however, based on other parameters (shown in Table 1B), we chose PLS-3 as a good model because it has a close agreement of fitting points on the regression line. Furthermore, when comparing AutoQSAR and 3D-QSAR, the predicted activities from 3D-QSAR have nearly identical values and a high degree of agreement between fitting points on the regression line. As a result, we chose the Gaussian-based 3D-QSAR model as the final model for further investigation.

Table 1: The experimental activity (activity-1) and predicted activity (PLS-4) with their structures, Ki values of test and training sets

Structure of the compound	Phase qsar set	Ki (nM)	Activity-1	Predicted Activity1	Predicted Activity2	Predicted Activity3	Predicted Activity4
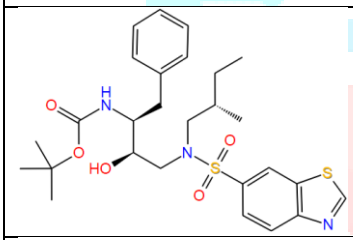	test	0.243	9.614	10.504	10.125	10.089	10.307
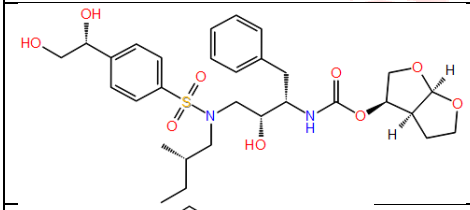	training	0.216	9.666	10.417	9.32	9.698	9.685
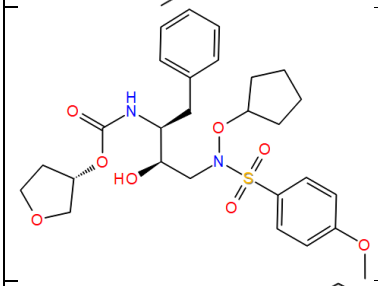	training	0.19	9.721	10.507	9.602	9.758	9.664
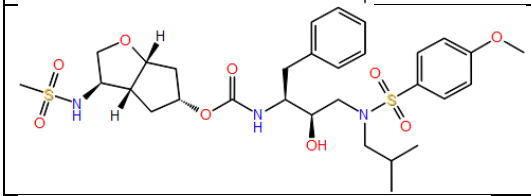	test	0.18	9.745	11.134	11.163	11.292	11.08
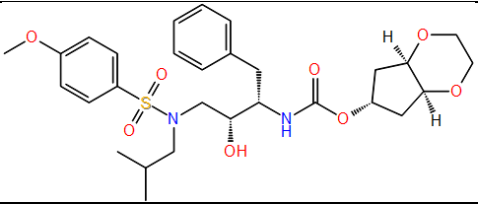	training	0.18	9.745	10.432	10.422	10.063	9.812

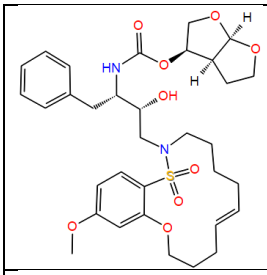	training	0.18	9.745	10.991	9.771	9.624	9.678
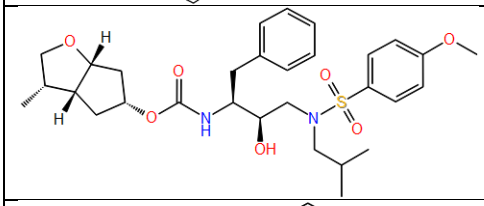	test	0.16	9.796	11.21	10.957	11.258	11.169
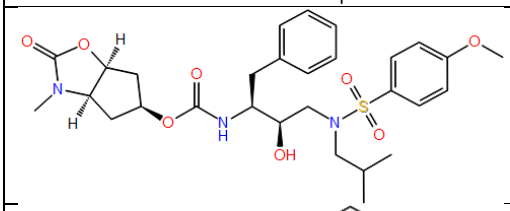	training	0.16	9.796	10.38	9.645	9.781	9.729
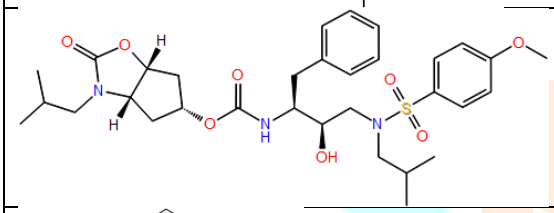	training	0.16	9.796	10.278	10.137	9.998	9.938
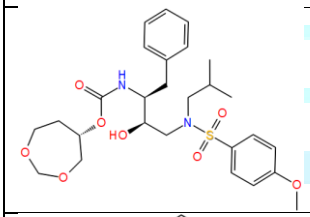	test	0.16	9.796	10.409	10.282	10.318	10.291
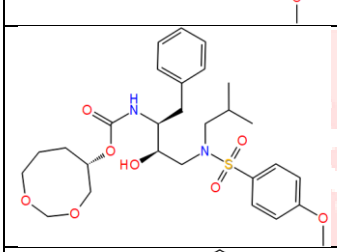	training	0.15	9.824	10.414	10.018	9.766	9.987
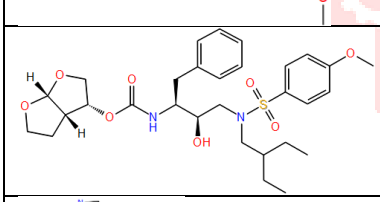	training	0.134	9.873	10.472	10.262	9.63	9.752
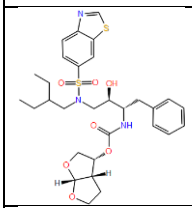	test	0.126	9.9	10.482	10.024	9.807	10.031
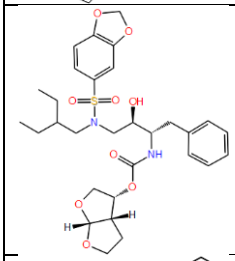	training	0.104	9.983	9.998	9.793	10	9.967
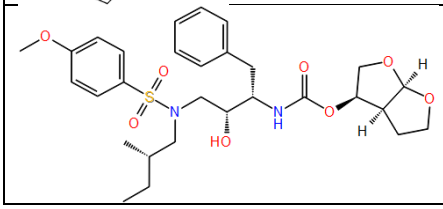	training	0.103	9.987	10.319	10.537	10.32	10.039

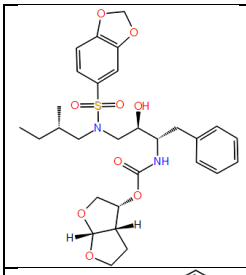	training	0.099	10.004	9.896	9.778	10.058	10.098
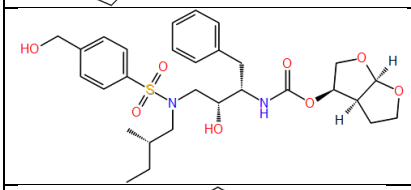	test	0.08	10.097	10.614	11.096	10.739	10.774
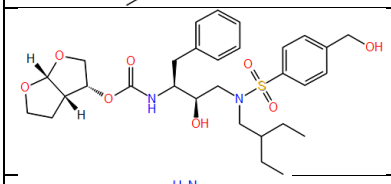	training	0.07	10.155	10.836	10.749	10.336	10.51
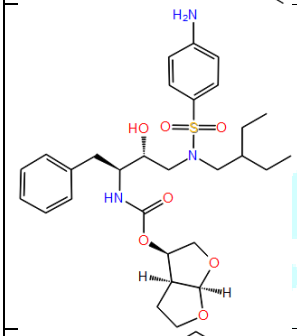	training	0.062	10.208	10.667	10.313	9.934	10.004
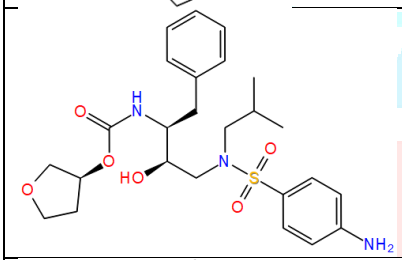	test	0.04	10.398	10.621	10.583	10.604	10.682
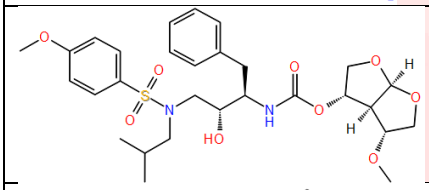	training	0.035	10.456	10.386	10.1	10.545	10.633
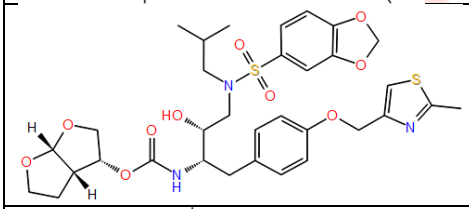	training	0.007	11.167	10.776	11.147	11.296	11.111
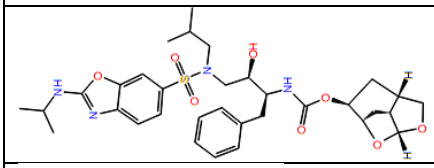	test	0.006	11.222	10.64	10.048	10.232	10.134
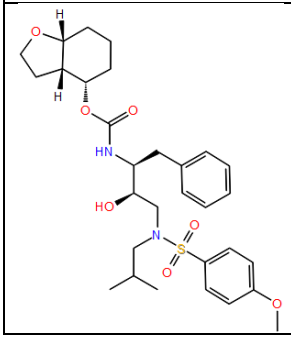	training	0.005	11.301	10.892	11.004	11.301	11.309

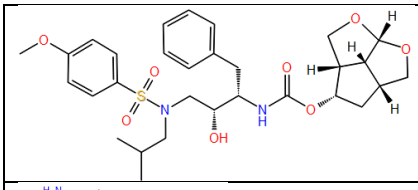	training	0.005	11.301	10.67	11.352	10.927	10.941
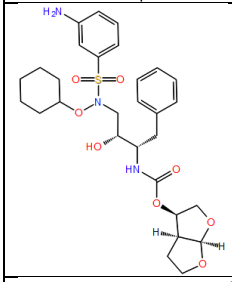	training	0.005	11.301	10.935	11.93	11.571	11.429
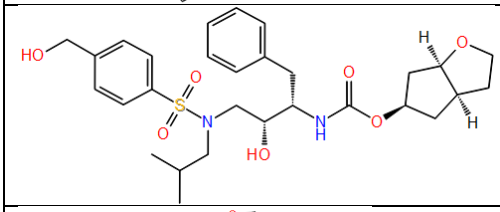	training	0.005	11.301	10.231	10.303	10.899	11.085
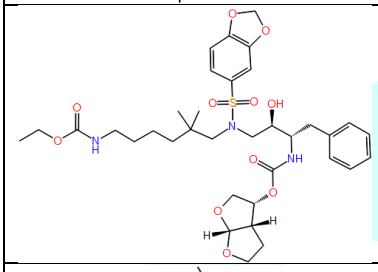	test	0.005	11.337	11.26	11.389	11.518	11.503
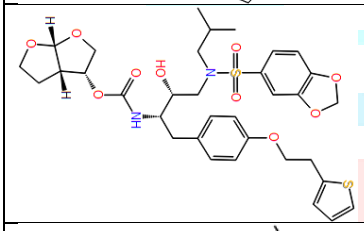	training	0.004	11.409	10.892	11.464	11.535	11.419
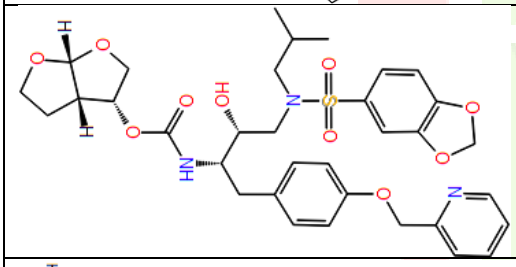	training	0.003	11.585	11.337	11.907	11.809	11.535
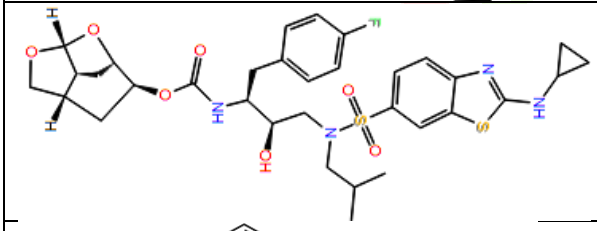	test	0.002	11.699	10.863	10.459	10.683	10.626
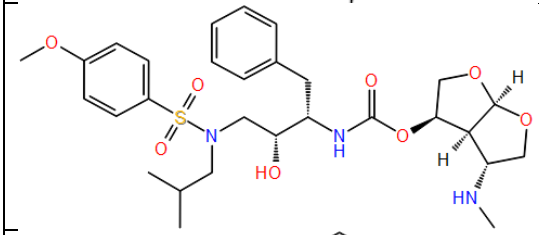	**training**	0.002	**11.824**	**11.659**	**11.756**	**11.787**	**11.682**
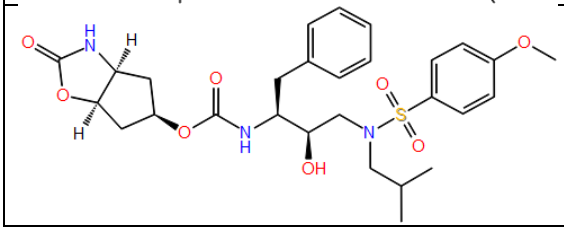	**test**	**0.001**	**11.921**	**10.741**	**11.331**	**10.932**	**10.879**

Table 2: Summary of QSAR models obtained from (A) AutoQSAR and [2] Gaussian-based 3D-QSAR

A

Model code	**Score**	**SD**	**R^2**	**RMSE**	**Q^2**	**Q^2 MW**
Kpls_linear_25	0.8739	0.4620	0.8864	0.4435	0.8519	0.5743
Kpls_molprint2D_14	0.8681	0.5021	0.8652	0.4190	0.8739	0.5509
Kpls_linear_24	0.8588	0.5196	0.8554	0.4334	0.8680	0.4749
Kpls_dendritic_25	0.8259	0.5332	0.8478	0.5182	0.8114	0.4739
Kpls_dendritic_24	0.8188	0.4733	0.8802	0.5003	0.8202	0.5509

B

ID	SD	R^2	R^2 CV	F	P	RMSE	Q^2	Pearson-r
PLS-1	0.9146	0.5344	0.2961	33.3	3.00E-06	0.66	0.7133	0.8482
PLS-2	0.6328	0.7848	0.3686	51.1	4.57E-10	0.69	0.6839	0.8745
PLS-3	0.4536	0.8934	0.3775	75.4	3.03E-13	0.65	0.721	0.8837
PLS-4	0.2925	0.9573	0.4149	145.7	2.11E-17	0.7	0.6787	0.8665
PLS-5	0.2175	0.9773	0.4343	215.2	1.05E-19	0.68	0.6953	0.8619

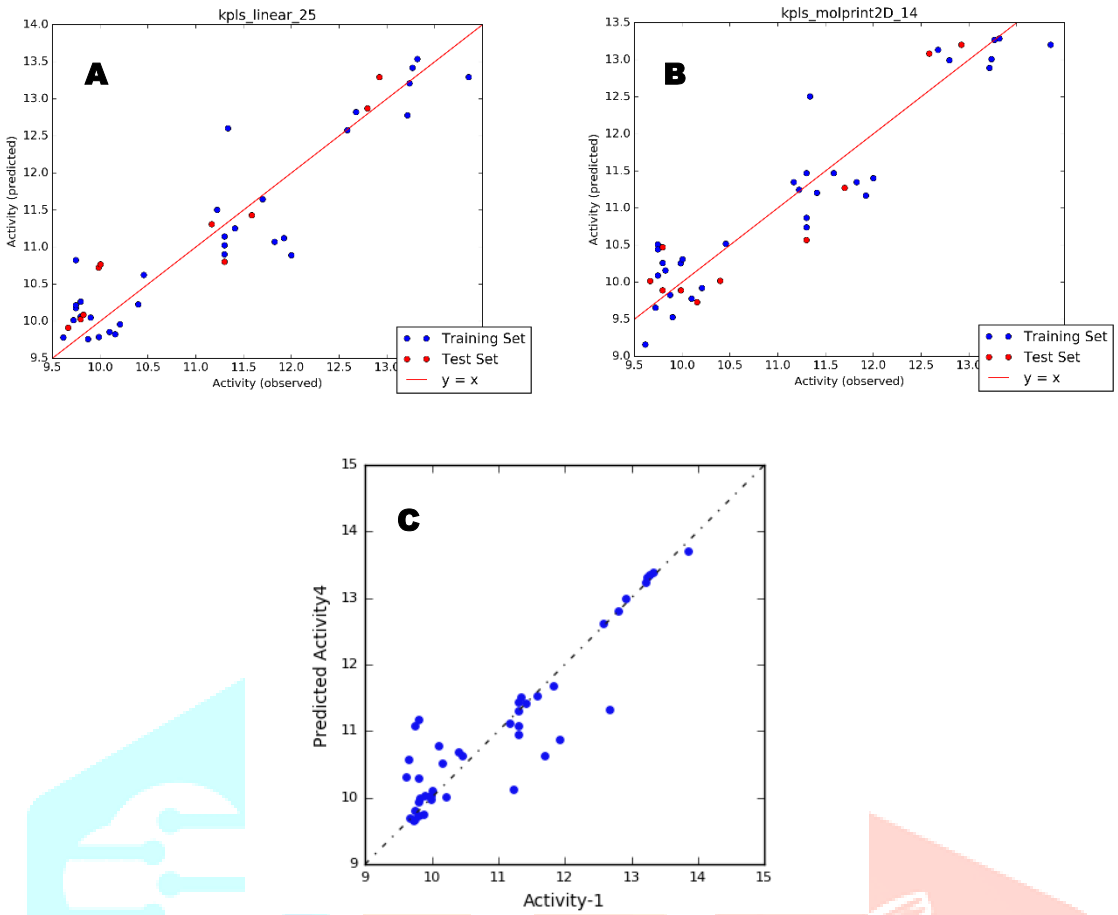

Figure 2: Plot shows the experimental activity versus predicted activity; (A, B) obtained from AutoQSAR [3] and (C) obtained from Gaussian based 3D-QSAR model (PLS-3).

A QSAR model based on Gaussian calculations was developed by determining the field-based fractions, including steric, electrostatic, hydrophobic, hydrogen bond donor (HBD), and hydrogen bond acceptor (HBA), and the biological activity of the compounds being studied. The PLS method was utilized to calculate the cross-validated correlation coefficient and other statistical measurements. The steric and electrostatic, hydrophobic, HBA, and HBD models contributed 0.383, 0.104, 0.201, 0.209, and 0.101, respectively. The 3D-QSAR model based on Gaussian demonstrated excellent predictive capability and furnished comprehensive insights into the structural attributes of molecules that contribute to their inhibitory activity. Additionally, the validation of the Gaussian-based 3D-QSAR model involved the creation of a graph that compared the predicted and experimental activity of both the training and test sets. To generate the Gaussian-based 3D QSAR contours maps, the compounds with the highest potency (**Figure 3**) were utilized. The Gaussian-based QSAR model utilized the five PLS factors derived from the **figure 3**. The contours maps reveal that the green-colored region signifies a favorable location for steric group substitution, which has the potential to enhance the activity. Specifically, the methoxy phenyl, sulfone, keto, and alkene groups are surrounded by green color contours, indicating that the presence of a steric group in these positions may lead to an increase in HIV-1 protease inhibition. It is worth noting that neither of these two molecules exhibits any yellow-colored contours on any groups, confirming that no group is likely to diminish the activity. The molecular structure is indicated by electrostatic contours in blue and red colors, representing electropositive and electronegative groups respectively. The blue region signifies a more favorable location for group/atom substitution, while the red surface indicates an unfavorable one. Both molecules have a significant red surface, suggesting that substituting electronegative atoms/groups in those regions may result in decreased activity. The hydrophobic maps display the preferred position with a yellow contour, while the unfavorable position is represented by a white contour for hydrophobic substitution. Additionally, the HBA contour map highlights the significant red surface indicating HBA groups that can enhance the activity. Conversely, the presence of magenta over phenyl and alkene groups will diminish the corresponding activity. The final contour map for HBD displays the blue-violet color to indicate an increase in HIV-protease activity due to the presence of HBD groups. On the other hand, the cyan contours suggest that HBD groups at these specific positions may potentially decrease the activity.

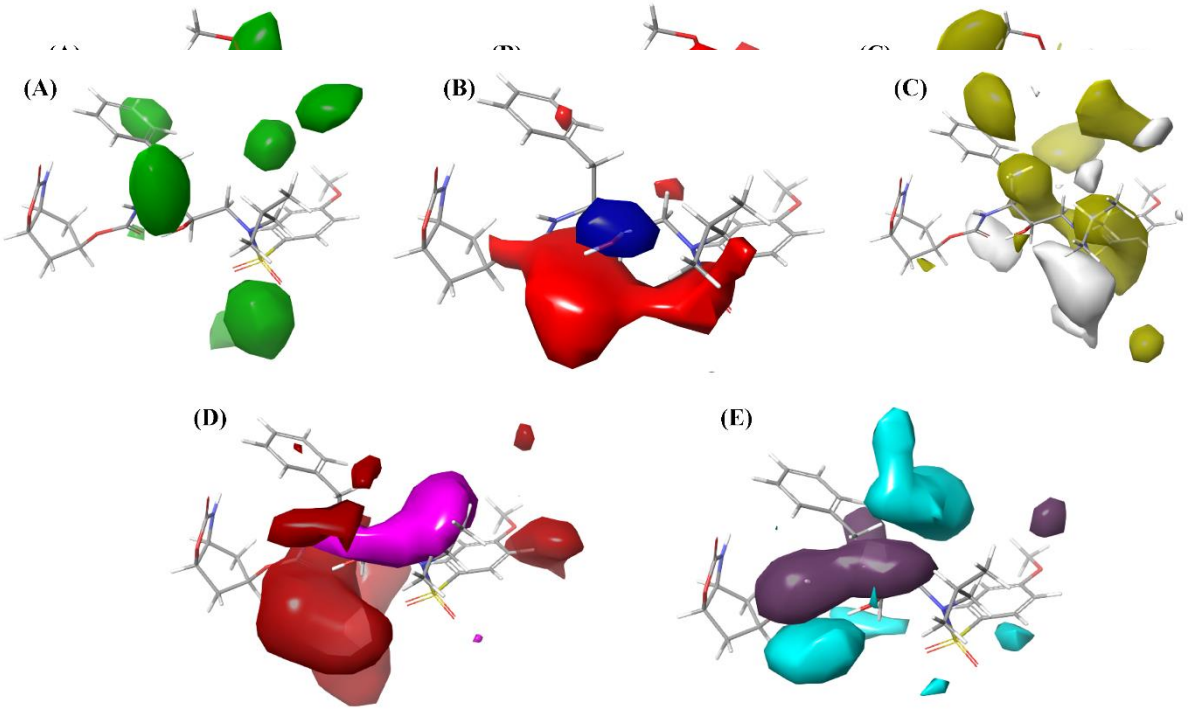

Figure 3: Pictorial representation of contribution of different kind of favorable and unfavorable features of most active compounds 32 and 33 (bottom) obtained from Gaussian based 3D-QSAR model.

The findings revealed that the compound **32 and 33** (**Figure 4**) exhibits a higher score compared to darunavir. The dataset utilized for this analysis consisted of 44 ligands, which were divided into training and testing sets for accurate evaluation. The biological activity of the darunavir molecule is significantly enhanced by the presence of a methoxy group at the position of the amine group, as indicated by the structure-activity relationship analysis of the compound series. Darunavir facilitates convenient entry into various derivatives that could potentially possess enhanced antiretroviral properties. Extensive research on the HIV protease-Darunavir complex has identified four crucial motifs encompassing the key hydroxyethyl isostere of Darunavir, known as the P1/P1' and P2/P2' moieties [23] (**Figure 5**). These moieties regulate the inhibitor precise interaction within the protease active site. Additional insight into an inhibitory activity can be gained by visualizing the QSAR model in the context of most active compounds. The drawn contour maps allow identification of those positions that require a particular physicochemical property to enhance the bioactivity of a ligand. The AutoQSAR model that has been validated as a search tool to retrieve compounds from the binding database. It is worth noting that the darunavir molecule exhibits strong interaction with the active site of the HIV-1 protease cavity, making it a well-known and highly effective inhibitor. Following this, the manually screened top candidate compound **32 and 33**, which possessed the highest predicted activity values, was carefully examined to identify potential inhibitors. Throughout this process, the overall structural information of the active site, the predicted activity value, and the physicochemical properties were taken into consideration. By utilizing physiochemical and topological descriptors, the study developed 2D and 3D-QSAR models that can predict the HIV-1 protease activities of dataset obtained from a binding database. The final models yield properties that capture the optimal Gaussian-based steric, electrostatic, hydrophobic, HBA, and HBD attributes of the highest ranked predicted compounds. The findings of this study offer valuable understanding of the molecular structural elements associated with inhibitory activities.

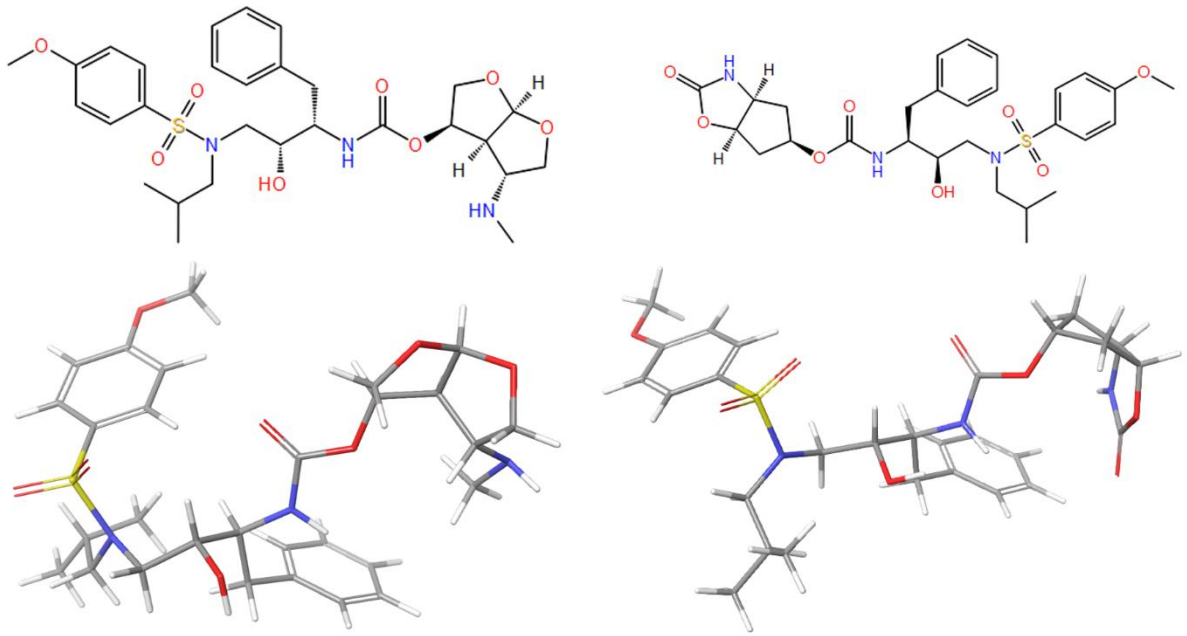

Figure 4: Chemical structure of most active compounds 32 (left) and 33 (right).

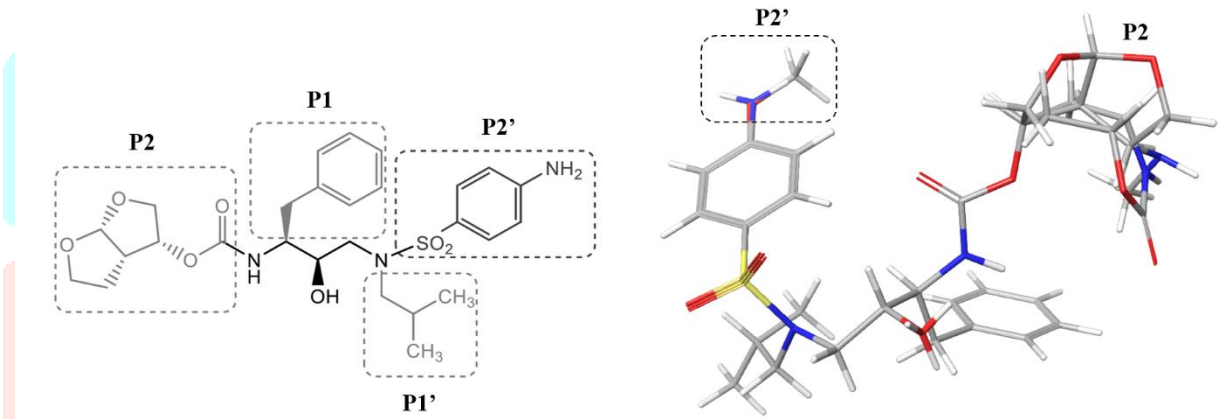

Figure 5: Chemical structure of darunavir and the superposition of compound 32 and 33 with darunavir to show the modified moieties in the P2/P2' section.

Molecular docking

Binding score and mode: To comprehend the binding mode and intermolecular interactions of the dataset employed for QSAR studies, it was subjected to docking within the binding site of HIV-1 protease. Consequently, molecular docking provides a significant means to characterize the binding capabilities of the ligands. Following the docking analysis, various scoring functions are utilized to assess the precision of protein-ligand complexes. The docking pose of each conformation is then ranked according to their score value and interactions. The optimal conformation for each compound was determined based on their docking score and glide energy. Compound-33 exhibited a docking score of -14.549 and a glide energy of -89.482 kcal/mol, while compound-32 had a docking score of -14.203 and a glide energy of -89.294 kcal/mol. These values are significantly higher than the values for darunavir, which had a docking score of -10.012 and a glide energy of -70.903 kcal/mol.

***Intermolecular Interactions*:** The molecular recognition process heavily relies on intermolecular interactions, which are characterized by attractive or repulsive forces between non-bonded atoms. These interactions, including hydrogen bonding, van der Waals forces, hydrophobic/hydrophilic interactions, electrostatic interactions, and halogen bonding, play a crucial role in the binding between DNA/protein and ligands. In **Figure 6,** we can observe the planar view of the intermolecular interactions within the complexes. The interaction between the amine group of the P2 moiety in darunavir and ASP30 can be observed in Compound-33 and Compound-32 after modification to a methoxy group. Additionally, darunavir forms hydrogen bonds with Arg8, Asp25, and Asp30. In contrast, Compound-32 and

Compound-33 exhibit stronger hydrogen bonding interactions with Arg8, Asp25, Asp29, Asp30, Ash25, and Gly48, indicating a stronger binding affinity compared to darunavir. All three molecules have well fitted in the active site of HIV-1 protease which confirms that the molecules form different type of intermolecular interactions such as conventional hydrogen bonding, carbon hydrogen bonding, hydrophobic and electrostatic interactions. It is important to note that lower values indicate stronger binding, as the binding energy is negative. Therefore, the strong binding of Compound-33 and Compound-32 to HIV-1 protease is evident from their highly negative binding energies. The binding energies for these complexes were determined to be -104.26 and -94.91 kcal/mol, respectively. These results confirm that the binding free energy of these complexes favours interactions with HIV-1 protease more effectively than darunavir, which has a binding energy of -70.903 kcal/mol. This suggests that the darunavir complex forms fewer interactions, resulting in lower binding energy and affinity. Furthermore, by altering the chemical structures within Compound-33 and Compound-32, the suppression of HIV-1 protease activity can be significantly improved.

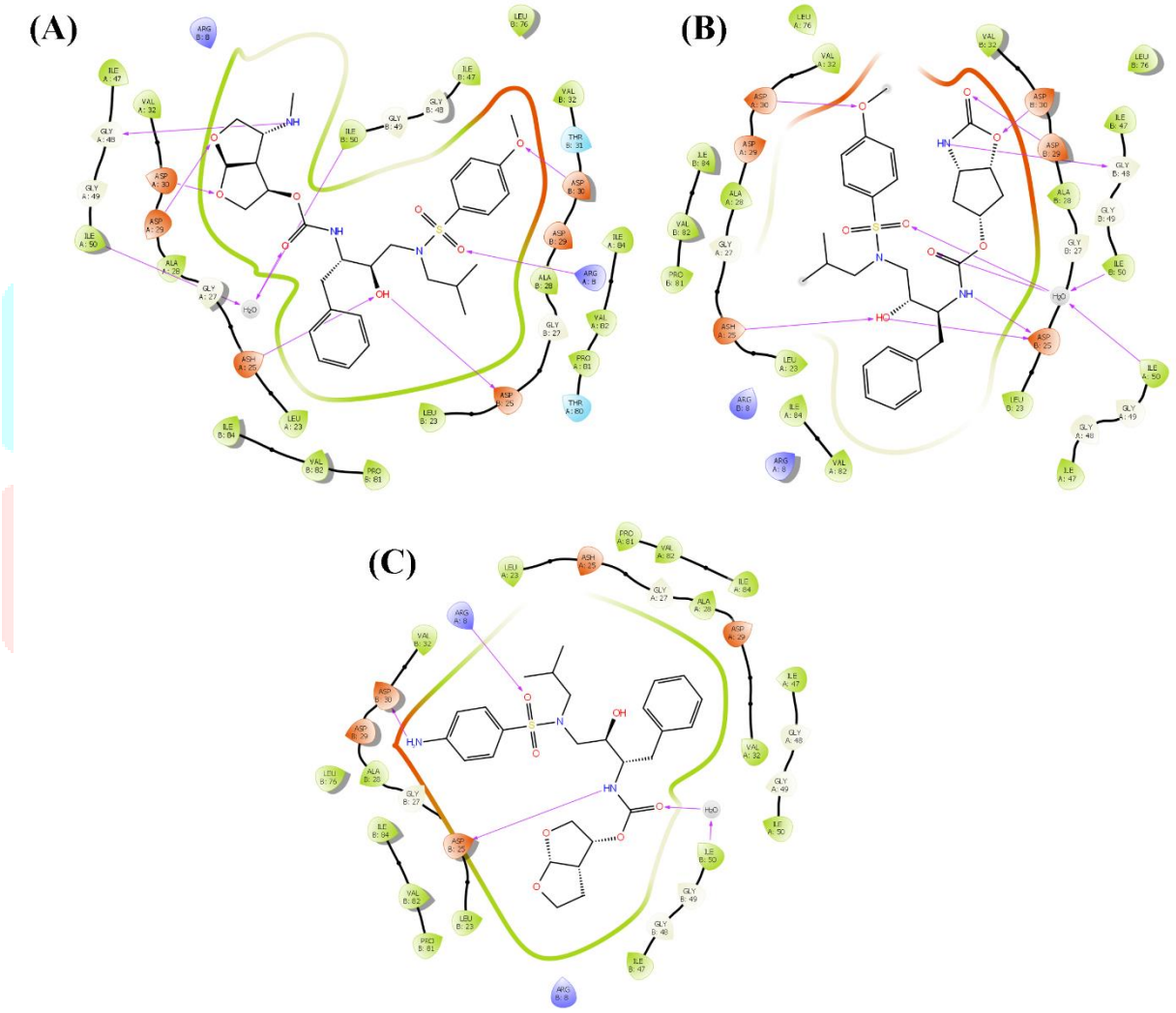

Figure 6: 2D view of Intermolecular interactions observed in the complexes, (A) compound-32; compound-33 and [3]Darunavir in the active site residues of HIV-1 protease.

4. Summary and Conclusion

We performed AutoQSAR and Gaussian-based 3D-QSAR analysis on an extremely diverse dataset of 44 inhibitors in this part. Following these findings, molecular docking was used to identify compound against HIV-1 protease. Furthermore, utilizing both the training and test sets, the most effective QSAR models were used to develop a Kernel PLS model. We were also able to visualize the contribution maps of the validated QSAR models using this method. The generated steric and electrostatic, hydrophobic, HBA, and HBD models serve as a structural foundation for the development of novel compounds and aid in understanding the fluctuations in their activity. Furthermore, predicted activity of the compounds closely matches their experimental activities, making it easier to identify new chemical entities with increased inhibition. The compound 32 and 33 carries higher potential activity

than darunavir, as shown by the molecular docking screening results, which agree with the QSAR studies. It is noteworthy that the structure-activity relationship analysis of the compound series indicates that the darunavir molecule is greatly enhanced by the presence of a methoxy group at the amine group position.

References

[1] L.M. Agosto, P. Zhong, J. Munro, W. Mothes, Highly active antiretroviral therapies are effective against HIV-1 cell-to-cell transmission, PLoS pathogens 10(2) (2014) e1003982.
[2] B.K. Ganser-Pornillos, M. Yeager, W.I. Sundquist, The structural biology of HIV assembly, Current opinion in structural biology 18(2) (2008) 203-217.
[3] Z. Lv, Y. Chu, Y. Wang, HIV protease inhibitors: a review of molecular selectivity and toxicity, HIV/AIDS-Research and palliative care (2015) 95-104.
[4] A.K. Ghosh, I.T. Weber, H. Mitsuya, Beyond darunavir: recent development of next generation HIV-1 protease inhibitors to combat drug resistance, Chemical Communications 58(84) (2022) 11762-11782.
[5] C. Nantasenamat, C. Isarankura-Na-Ayudhya, V. Prachayasittikul, Advances in computational methods to predict the biological activity of compounds, Expert opinion on drug discovery 5(7) (2010) 633-654.
[6] E.N. Muratov, J. Bajorath, R.P. Sheridan, I.V. Tetko, D. Filimonov, V. Poroikov, T.I. Oprea, I.I. Baskin, A. Varnek, A. Roitberg, QSAR without borders, Chemical Society Reviews 49(11) (2020) 3525-3564.
[7] F.A. Olotu, C. Agoni, O. Soremekun, M.E.S. Soliman, The recent application of 3D-QSAR and docking studies to novel HIV-protease inhibitor drug discovery, Expert Opinion on Drug Discovery 15(9) (2020) 1095-1109.
[8] Z. Ul-Haq, S. Usmani, H. Shamshad, U. Mahmood, S.A. Halim, A combined 3D-QSAR and docking studies for the In-silicoprediction of HIV-protease inhibitors, Chemistry Central Journal 7(1) (2013) 1-12.
[9] J. Tong, Y. Wu, M. Bai, P. Zhan, 3D-QSAR and molecular docking studies on HIV protease inhibitors, Journal of Molecular Structure 1129 (2017) 17-22.
[10] J. Vora, S. Patel, S. Sinha, S. Sharma, A. Srivastava, M. Chhabria, N. Shrivastava, Molecular docking, QSAR and ADMET based mining of natural compounds against prime targets of HIV, Journal of Biomolecular Structure and Dynamics 37(1) (2019) 131-146.
[11] M. Baassi, M. Moussaoui, H. Soufi, S. Rajkhowa, A. Sharma, S. Sinha, S. Belaaouad, Towards designing of a potential new HIV-1 protease inhibitor using QSAR study in combination with Molecular docking and Molecular dynamics simulations, Plos one 18(4) (2023) e0284539.
[12] M.H. Fatemi, A. Heidari, S. Gharaghani, QSAR prediction of HIV-1 protease inhibitory activities using docking derived molecular descriptors, Journal of Theoretical Biology 369 (2015) 13-22.
[13] N. Saranya, S. Selvaraj, QSAR studies on HIV-1 protease inhibitors using non-linearly transformed descriptors, Current computer-aided drug design 8(1) (2012) 10-49.
[14] R. Garg, S.P. Gupta, H. Gao, M.S. Babu, A.K. Debnath, C. Hansch, Comparative quantitative structure–activity relationship studies on anti-HIV drugs, Chemical reviews 99(12) (1999) 3525-3602.
[15] K. Takkis, S. Sild, QSAR Modeling of HIV-1 Protease Inhibition on Six-and Seven-membered Cyclic Ureas, QSAR & Combinatorial Science 28(1) (2009) 52-58.
[16] A.K. Halder, T. Jha, Validated predictive QSAR modeling of N-aryl-oxazolidinone-5-carboxamides for anti-HIV protease activity, Bioorganic & medicinal chemistry letters 20(20) (2010) 6082-6087.
[17] A.C. Nair, P. Jayatilleke, X. Wang, S. Miertus, W.J. Welsh, Computational studies on tetrahydropyrimidine-2-one HIV-1 protease inhibitors: improving three-dimensional quantitative structure− activity relationship comparative molecular field analysis models by inclusion of calculated inhibitor-and receptor-based properties, Journal of medicinal chemistry 45(4) (2002) 973-983.
[18] A.S. Reddy, S. Kumar, R. Garg, Hybrid-genetic algorithm based descriptor optimization and QSAR models for predicting the biological activity of Tipranavir analogs for HIV protease inhibition, Journal of Molecular Graphics and Modelling 28(8) (2010) 852-862.
[19] P. Nunthanavanit, N.G. Anthony, B.F. Johnston, S.P. Mackay, J. Ungwitayatorn, 3D-QSAR Studies on Chromone Derivatives as HIV-1 Protease Inhibitors: Application of Molecular Field Analysis, Archiv der Pharmazie: An International Journal Pharmaceutical and Medicinal Chemistry 341(6) (2008) 357-364.
[20] S. Durdagi, T. Mavromoustakos, M.G. Papadopoulos, 3D QSAR CoMFA/CoMSIA, molecular docking and molecular dynamics studies of fullerene-based HIV-1 PR inhibitors, Bioorganic & medicinal chemistry letters 18(23) (2008) 6283-6289.
[21] T. Liu, Y. Lin, X. Wen, R.N. Jorissen, M.K. Gilson, BindingDB: a web-accessible database of experimentally determined protein–ligand binding affinities, Nucleic acids research 35(suppl_1) (2007) D198-D201.
[22] S.L. Dixon, J. Duan, E. Smith, C.D. Von Bargen, W. Sherman, M.P. Repasky, AutoQSAR: an automated machine learning tool for best-practice quantitative structure–activity relationship modeling, Future medicinal chemistry 8(15) (2016) 1825-1839.
[23] J.L. Paulsen, F. Leidner, D.A. Ragland, N. Kurt Yilmaz, C.A. Schiffer, Interdependence of inhibitor recognition in HIV-1 protease, Journal of chemical theory and computation 13(5) (2017) 2300-2309.